Title	Fully analytic valence force field model for the elastic and inner elastic properties of diamond and zincblende crystals
Authors	Tanner, Daniel S. P.;Caro, Miguel A.;Schulz, Stefan;O'Reilly, Eoin P.
Publication date	2019-09-30
Original Citation	Tanner, D. S. P., Caro, M. A., Schulz, S. and O'Reilly, E. P. (2019) 'Fully analytic valence force field model for the elastic and inner elastic properties of diamond and zincblende crystals', Physical Review B, 100(9), 094112, (14pp). doi: 10.1103/PhysRevB.100.094112
Type of publication	Article (peer-reviewed)
Link to publisher's version	https://link.aps.org/doi/10.1103/PhysRevB.100.094112 - 10.1103/PhysRevB.100.094112
Rights	
Download date	2025-07-18 06:26:08
Item downloaded from	https://hdl.handle.net/10468/8852

Fully analytic valence force field model for the elastic and inner elastic properties of diamond and zincblende crystals

Daniel S. P. Tanner,[1,*] Miguel A. Caro,[2,3] Stefan Schulz,[1] and Eoin P. O'Reilly[1,4]

[1]*Tyndall National Institute, Lee Maltings, Dyke Parade, Cork T12 R5CP, Ireland*
[2]*Department of Electrical Engineering and Automation, Aalto University, Espoo 02150, Finland*
[3]*Department of Applied Physics, Aalto University, Espoo 02150, Finland*
[4]*Department of Physics, University College Cork, Cork T12 YN60, Ireland*

Using a valence force field model based on that introduced by Martin, we present three related methods through which we analytically determine valence force field parameters. The methods introduced allow easy derivation of valence force field parameters in terms of the Kleinman parameter ζ and bulk properties of zincblende and diamond crystals. We start with a model suited for covalent and weakly ionic materials, where the valence force field parameters are derived in terms of ζ and the bulk elastic constants C_{11}, C_{12}, and C_{44}. We show that this model breaks down as the material becomes more ionic and specifically when the elastic anisotropy factor $A = 2C_{44}/(C_{11} - C_{12}) > 2$. The analytic model can be stabilized for ionic materials by including Martin's electrostatic terms with effective cation and anion charges in the valence force field model. Inclusion of effective charges determined via the optical phonon mode splitting provides a stable model for all but two of the materials considered (zincblende GaN and AlN). A stable model is obtained for all materials considered by also utilizing the inner elastic constant E_{11} to determine the magnitude of the effective charges used in the Coulomb interaction. Test calculations show that the models describe well structural relaxation in superlattices and alloys and reproduce key phonon band structure features.

I. INTRODUCTION

The use of interatomic potentials for the study of the elastic properties of solids has a long history. Relations between the elastic constants of crystals were obtained as early as the 19th century [1], when the Cauchy relations were derived analytically using a simple central pairwise atomic interaction. Later it was found by Born that in order to model covalent crystals, whose elastic constants do not bear such simple relation to each other, noncentral interatomic interactions needed to be included [2]. In this manner the complexity of the involved potentials grew with the variety of systems to which they were applied, with today's interatomic potentials involving up to hundreds of different atomic interactions, parametrized and implemented at great computational expense [3,4].

Generally, interatomic potentials were used to predict unknown crystal properties from known ones. For example, in the early literature, interatomic potentials parametrized from known elastic constants (for example C_{11} and C_{12}) or phonon frequencies were used to predict such experimentally inaccessible quantities as inner elastic constants and internal strain [2,5–7], temperature, pressure and strain dependence of elastic constants [8–10], third order elastic constants [5,10], vibrational properties [11–13], as well as to gain general insights into interatomic forces, and explanations for trends in elastic properties [5,14,15].

More recently, with the advent of *ab initio* calculations, capable of determining all *bulk* elastic, inner elastic, and dynamical properties of a crystal to a high accuracy, the use of interatomic potentials for the prediction of the properties of simple bulk systems has dropped off: While the predictions of interatomic potentials were useful first approximations, their use was no longer justified when such properties could be easily calculated to a high accuracy using first-principles methods. Furthermore, properties such as the previously experimentally inaccessible internal relaxation and various shear moduli, which were formerly predicted by interatomic potentials, may now be used in their parametrization [16].

This has led to the contemporary use of interatomic potentials to be predominantly in the calculation of the properties of larger nonhomogeneous systems, which *cannot* be modelled using a small periodic cell, and for which *ab initio* calculations are not computationally feasible. The calculation of the strain and relaxed atomic positions of large supercells is of crucial importance to the semiconductor science community [17,18]. This is because the electronic and optical properties of heterostructures are strongly influenced by their strain state [19]. Furthermore, computationally cheaper continuum models are able to account for neither the atomic-scale variation of composition, nor the atomic-scale reduction in symmetry which have significant effects on electronic properties [20,21].

We present here a set of potential models which are ideally suited to the study of such structures. The valence force field (VFF) model that we use is based on that introduced by Martin [14]. It is well established how to determine both macroscopic elastic constants and quantities such as internal

---

elastic constants and the Kleinman parameter from a given set of VFF parameters. We show here that it is possible for diamond and zincblende (ZB) structures to solve the inverse problem, namely to calculate VFF parameters for a given material based on known elastic constant and internal strain values. The analysis also derives stability criteria for different versions of the VFF model, allowing a simple but accurate model for covalent and weakly ionic materials, with additional Coulombic terms required for more ionic materials. Having introduced the different models, we then use the results of previous *ab initio* density functional theory calculations to derive and present VFF parameter sets for a series of III-V ZB materials. The VFF models presented are straightforward to implement in existing atomic simulation packages such as LAMMPS [22] and GULP [23], thereby allowing the calculation of atomic relaxation and strain with a high degree of accuracy, efficiency, and physical clarity.

The potential best known for analytic calculation of parameters is that of Keating [5]. This uses only two VFF parameters, which are determined analytically from the elastic constants C_{11} and C_{12}. The model then describes those two parameters exactly and captures other elastic properties/constants reasonably well. In diamond structure Si, for example, the Keating potential will give exact C_{11} and C_{12}, and C_{44} with a 1% error [5]. Furthermore, while the Keating potential is limited to modelling a particular strain regime of a particular crystal phase, it is not, due to the analytic expressions for the force constants, limited to any particular material. In addition to the accuracy, efficiency, and cross-material transferability exhibited by the Keating potential and others in its class, the simplicity of these models allows not only for the prediction of the behavior of large complicated systems – but also for its explanation. Because of these advantages, the Keating potential remains widely used for the calculation of strain and atomistic relaxation in large systems, such as semiconductor quantum dots comprising millions of atoms [24–27].

Unfortunately, to describe the elasticity of cubic crystals fully requires more than two elastic constants (and more than two force constants), and the Keating potential fares less well for materials other than Si. For heteropolar materials (e.g., GaAs, InAs) errors in C_{44} grow with ionicity, and these errors manifest in the inaccurate modeling of systems where shear strains or internal relaxations are important [20,25,26].

The model that we present here, by including details of the inner elasticity of ZB and diamond crystals, improves on the accuracy of the Keating model for the description of the elasticity of ZB and diamond structure materials, but retains a simple analytic relation between the potential force constants and the elastic properties of the material. The model possesses the following attractive features: (i) it can be immediately applied to any diamond or ZB structure material for which the required elastic constants are known, with no numerical fitting required; (ii) it offers an exact description of C_{11}, C_{12}, C_{44}, and the Kleinman parameter ζ, thus providing significantly improved accuracy over the traditional Keating model, as well as the advantages of improved accuracy and computational efficacy over more complex potentials; (iii) analytic expressions for the force constants allow for clear interpretation and explanation of results, as well as *a priori* prediction of crystal properties other than those by which the potential was

parametrized; (iv) as noted above, the simple functional form of the potential is available in most molecular dynamics or crystal energy packages, such as LAMMPS or GULP (unlike the squared dot products of the Keating model), meaning that anyone with access to these or similar packages can use the potential immediately.

In the next section, the elasticity of ZB and diamond structure crystals is described, followed in Sec. III by an outline of the method by which the force constants of an interatomic potential may be analytically related to the constants governing the elastic response of any ZB or diamond crystal. We then present in Sec. III A the solution of the inverse problem for the covalent model, and an investigation of the stability of the covalent model for the III-V materials considered, with further details of the analysis included in the Appendix. Sections III B and III C introduce electrostatic interactions into the VFF model, with the values of the effective charges determined from the measured optical phonon splitting for each material in Sec. III B and using the internal elastic constant E_{11} in Sec. III C. In Sec. IV, the potentials are benchmarked against first principles and experimental results. Finally, the results are summarized and conclusions presented in Sec. V.

II. THEORY

The primitive unit cell of a ZB or diamond crystal is shown in Fig. 1. The cell consists of two interpenetrating face centered cubic lattices. The cell can be strained as a whole, and displacements can also occur between the sublattices, known as *internal strain* [2,6]. In the harmonic regime macroscopic distortions of the whole cell are completely specified by the strain tensor ε, and the internal strain between the sublattices is specified by the internal strain vector **u**.

The free energy per unit mass per unit volume of a ZB or diamond crystal for a general state of (small) macroscopic and internal strain consistent with its cubic symmetry is
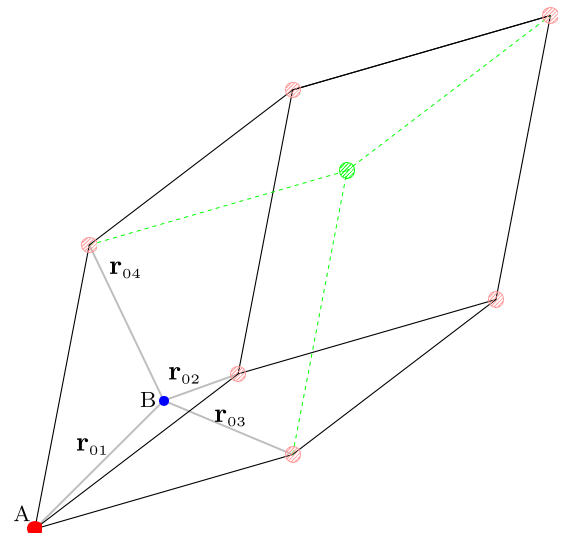

FIG. 1. Zincblende primitive cell.

given by:

$$U = \tfrac{1}{2}C_{11}\big(\varepsilon_1^2 + \varepsilon_2^2 + \varepsilon_3^2\big) + C_{12}(\varepsilon_1\varepsilon_2 + \varepsilon_1\varepsilon_3 + \varepsilon_2\varepsilon_3)$$
$$+ \tfrac{1}{2}C_{44}^0\big(\varepsilon_4^2 + \varepsilon_5^2 + \varepsilon_6^2\big) + D_{14}(u_x\varepsilon_4 + u_y\varepsilon_5 + u_z\varepsilon_6)$$
$$+ \tfrac{1}{2}E_{11}\big(u_x^2 + u_y^2 + u_z^2\big). \tag{1}$$

Here the notation of Cousins [6,10,28] is utilized for the elastic and inner elastic constants, and we have also above employed Voigt [29,30] notation, which, using the symmetry of the strain tensor, makes the convenient contraction of indices: $11 \to 1$, $22 \to 2$, $33 \to 3$, $23 \to 4$, $13 \to 5$, $12 \to 6$. In the above equation C_{11} and C_{12} are the familiar second-order elastic constants of a cubic crystal, which may be readily obtained from experiment, while C_{44}^0 is the experimentally unobtainable unrelaxed or "bare" C_{44} (also known as the clamped-ion contribution to the elastic constant C_{44} [31,32]); C_{44}^0 governs how the crystal responds to shear strains when the internal strain is set equal to zero. The constant D_{14} accounts for coupling between internal and macroscopic strain, and the term E_{11} describes the contribution to the free energy from a pure internal strain.

E_{11} may be related to the zone-center transverse optical phonon frequency and can thus be obtained indirectly from experiment. This relation is given by [16,28,31]:

$$E_{11} = 4\mu\omega_{\mathrm{TO}}^2/a_0^3, \tag{2}$$

where μ is the reduced mass of the anion and cation system, ω_{TO} is the transverse optical phonon frequency at Γ, and a_0 is the lattice constant. The remaining two constants, C_{44}^0 and D_{14}, may be obtained by considering the crystal energy once it is minimized with respect to internal strain, $\mathbf{u}$. The value of the internal strain which minimizes the free energy is given by:

$$\mathbf{u}^0 = \left(-\frac{a_0}{4}\zeta\varepsilon_4, -\frac{a_0}{4}\zeta\varepsilon_5, -\frac{a_0}{4}\zeta\varepsilon_6 \right), \tag{3}$$

where ζ is Kleinman's internal strain parameter [33], given by:

$$\zeta = \frac{\sqrt{3}}{r_0}\frac{D_{14}}{E_{11}}. \tag{4}$$

Though very difficult to perform, especially for more brittle crystals [28], measurements of the Kleinman parameter, ζ, have been made for a limited number of materials. For example, there are experimental values of the Kleinman parameter in the literature for Si [34], Ge [34], GaAs [35], C [36], and InSb [37]. However, reflecting a general trend for inner elastic properties, first principles determinations of the Kleinman parameter are abundant for most group IV or III-V cubic materials [31,38,39]. Substituting Eq. (3) into Eq. (1) then gives the familiar expression for the free energy which is minimized with respect to internal strain:

$$U = \tfrac{1}{2}C_{11}\big(\varepsilon_1^2 + \varepsilon_2^2 + \varepsilon_3^2\big) + C_{12}(\varepsilon_1\varepsilon_2 + \varepsilon_1\varepsilon_3 + \varepsilon_2\varepsilon_3)$$
$$+ \tfrac{1}{2}C_{44}\big(\varepsilon_4^2 + \varepsilon_5^2 + \varepsilon_6^2\big), \tag{5}$$

where C_{44} is now the experimentally measurable C_{44}, reduced from its unrelaxed value by:

$$C_{44} = C_{44}^0 - \frac{D_{14}^2}{E_{11}} = C_{44}^0 - \frac{r_0^2}{3}\zeta^2 E_{11}. \tag{6}$$

Given the above dependencies amongst the relaxed and unrelaxed elastic constants, if any three independent constants (out of the five: C_{44}, ζ, E_{11}, D_{14}, C_{44}^0) are known, then the remaining two can be obtained indirectly. Likewise, if any interatomic potential is able to accurately model C_{11}, C_{12}, and three of these constants, then the free energy density under any combination of strain or sublattice displacement will be fully described.

To relate these components of the free energy density to the force constants of an interatomic potential, the interatomic potential is used to express the energy of an arbitrarily deformed primitive diamond or ZB cell. This energy is divided by the equilibrium cell volume to obtain the free energy density, and then the VFF energy, expressed naturally as a function of the distance between the two atoms in the primitive cell, is cast in terms of the strain and internal strain:

$$U^{\mathrm{VFF}}(r_{ij}, \theta_{ijk}) \Longrightarrow U^{\mathrm{VFF}}(\varepsilon, \mathbf{u}). \tag{7}$$

Here we have denoted the primitive cell energy density, expressed in terms of the VFF force constants as U^{VFF}. Generally, the expression of the VFF energy in terms of the strain and internal strain, $U^{\mathrm{VFF}}(\varepsilon, \mathbf{u})$, will be a very complicated and long function of ε. However, we are only interested in harmonic elastic properties, so it can therefore be expanded in a Taylor series about the equilibrium and truncated to second order.

To effect the transformation of Eq. (7), consider Fig. 1. Keeping the atom at the origin of the cell fixed, the interatomic bond lengths can be expressed in terms of the strain and internal strain through the transformation with strain of the atomic position vectors:

$$\mathbf{r}_A = \mathbf{r}_{A,0} = [0, 0, 0],$$
$$\mathbf{r}_B = (I + \varepsilon)\mathbf{r}_{B,0} + \mathbf{u}. \tag{8}$$

Here, $\mathbf{r}_A$ ($\mathbf{r}_B$) is the position of the atom labeled A (B) in Fig. 1, with $\mathbf{r}_{A,0}$ ($\mathbf{r}_{B,0}$) being the equilibrium position of this atom, and I is the 3×3 identity matrix. Substituting these position vectors into the expression for the VFF energy will give the energy in terms of the strain, which can then be truncated to second order. This procedure has been detailed by Keating [5].

Following this expansion, direct analytic relations between the elastic and inner elastic constants and the force constants may be obtained via the derivatives:

$$C_{11} = \frac{\partial^2 U^{\mathrm{VFF}}}{\partial\varepsilon_1^2}; \quad C_{12} = \frac{\partial^2 U^{\mathrm{VFF}}}{\partial\varepsilon_1\partial\varepsilon_2},$$

$$C_{44}^0 = \frac{\partial^2 U^{\mathrm{VFF}}}{\partial\varepsilon_4^2}; \quad D_{14} = \frac{\partial^2 U^{\mathrm{VFF}}}{\partial u_x\partial\varepsilon_4},$$

$$E_{11} = \frac{\partial^2 U^{\mathrm{VFF}}}{\partial u_x^2}; \quad C_{44} = \frac{\partial^2 U^{\mathrm{VFF}}(\mathbf{u} = \mathbf{u}_0)}{\partial\varepsilon_4^2},$$

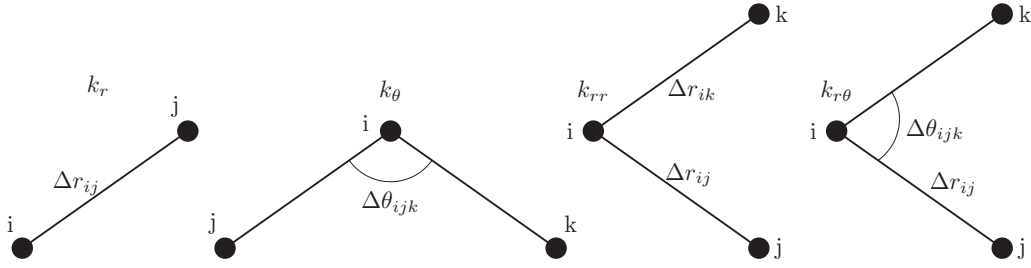$$\zeta = \frac{-4u_x^0(\varepsilon_4)}{a_0\varepsilon_4}. \tag{9}$$

FIG. 2. Valence force field interaction terms contributing to Eq. (10). From left to right: bond stretching, k_r; bond bending, k_θ; bond-bond stretching, k_{rr}; bond-stretching angle-bending coupling constant, $k_{r\theta}$.

In the next section, we present the VFF model with which we model the elastic energy density described above.

III. INTERATOMIC POTENTIAL

The VFF with which we describe the elastic properties of diamond and ZB crystals was originally introduced by Musgrave and Pople [11]. We shall follow the developments made on this potential by Martin [14]. Discarding a purportedly unimportant cross angle term, and including terms which account for the Coulomb interaction between the partially charged ions of a heteropolar crystal, Martin gives the form of the potential which will be used in this work. For each atom in a ZB crystal Martin's potential is given by:

$$
\begin{aligned}
V_i = {} & \frac{1}{2}\sum_{j\neq i}\frac{1}{2}k_r\big(r_{ij}-r_{ij}^0\big)^2 + \sum_{j\neq i}\sum_{k\neq i,k>j}\left\{\frac{1}{2}k_\theta^i r_{ij}^0 r_{ik}^0\big(\theta_{ijk}-\theta_{ijk}^0\big)^2\right. \\
& + k_{r\theta}^i\big[r_{ij}^0\big(r_{ij}-r_{ij}^0\big)+r_{ik}^0\big(r_{ik}-r_{ik}^0\big)\big]\big(\theta_{ijk}-\theta_{ijk}^0\big) \\
& \left.+ k_{rr}^i\big(r_{ij}-r_{ij}^0\big)\big(r_{ik}-r_{ik}^0\big)\right\} + \frac{1}{2}{\sum_{j\neq i}}'\frac{Z_i^* Z_j^* e^2}{4\pi\epsilon_r\epsilon_0 r_{ij}} \\
& - \frac{1}{2}\sum_{j\neq i}^{nn}\frac{1}{4}\alpha_M\frac{Z_i^* Z_j^* e^2}{4\pi\epsilon_r\epsilon_0 r_{ij}^{0\,2}}\big(r_{ij}-r_{ij}^0\big).
\end{aligned}
\tag{10}
$$

Here i refers to the central atom being considered, while j and k run over the four nearest neighbors for each i, except for the summation $\sum_{j\neq i}'$, which runs over the whole crystal. This means that in modeling the energy of a ZB or diamond primitive cell eight bond lengths and twelve angles will be treated. The half preceding all two body terms prevents double counting when summing over i, to obtain the energy of the whole crystal from the energy per atom. $r_{ij}=(\mathbf{r}_{ij}\cdot\mathbf{r}_{ij})^{\frac{1}{2}}$ refers to the bond length between atom i and j, $\theta_{ijk}=\cos^{-1}\left(\frac{\mathbf{r}_{ij}\cdot\mathbf{r}_{ik}}{|\mathbf{r}_{ij}||\mathbf{r}_{ik}|}\right)$ refers to the angle between the bonds r_{ij} and r_{ik}, and r_{ij}^0 and θ_{ijk}^0 denote the equilibrium bond lengths and bond angles, respectively.

The covalent potential terms of Eq. (10) are schematically illustrated in Fig. 2. The term k_r captures the resistance of any bond to length changes away from the equilibrium length, likewise k_θ^i describes the harmonic resistance to changes in angle. The term k_{rr}^i describes the relation between neighboring bonds which share an atom (atom i); how one bond will tend to increase in length if another is decreased. $k_{r\theta}^i$ describes the interaction between the angle between two bonds, and each of the two bonds; this will, for example, for $k_{r\theta}^i > 0$, make it en-

ergetically favorable for bond lengths to increase when bond angles decrease. This energetic favorability can be imputed to changes in the s-p mixing on the orbitals sitting on the central atom [40]. The amount by which the energy changes due to this rehybridization would in principle depend on the species of the central atom; which in turn would imply different three-body terms are needed for the cation and the anion, hence the superscript i on these terms. However, Martin justifies the exclusion of this effect by emphasizing that the potential is being used to study only phenomena in the long-wavelength regime: elastic properties, as well as zone center optic and acoustic modes. In this case the force constants for the two atoms in the unit cell always enter the energy and frequency equations together, and thus could not be separated, nor would treating them as different result in an improvement in the description of any of our targeted elastic constants. Anion-centered and cation-centered angular terms are thus treated as the same.

The last two terms in Eq. (10) account for electrostatic effects, with Z^* representing the effective charge of the ions and α_M denoting the Madelung constant. The first of these is the screened Coulomb interaction, and the second is a linear repulsive term, given by the linear part of the Taylor expansion of the Coulomb energy in the strain, necessary to keep the crystal stable at equilibrium, and also to preserve the symmetry of the elastic constant tensor. The prime symbol over the summation of Coulomb interaction indicates it is a long-ranged interaction which must be computed over the whole crystal.

In the work by Martin further approximations and dependencies were applied to the force constants such that Eq. (10) becomes equivalent to the Keating potential with additional Coulombic terms. In this work no dependencies amongst the force constants are imposed, and there are thus four force constants and an effective charge with which we can describe the elastic properties of diamond and ZB crystals. For the description of the elastic energy density given in Eq. (1), no advantage can be expected from including any further force constants in the VFF model, given the arbitrariness in choice of parameter values when fitting six or more VFF parameters to the five independent elastic constants.

To obtain the numerical values for the force constants in Eq. (10), the potential must be expanded after the manner of Keating, as described in Sec. II. However, this procedure is not straightforward for the Coulomb term; in this case a numerical Ewald summation must be performed for different strained crystal states to determine the dependence of the Coulomb energy of the whole crystal on strain. The expansion

of our potential in Eq. (10) in terms of strain and sublattice displacement is given in Eq. (11) below:

$$
\begin{aligned}
U &= \frac{\sqrt{3}}{2}\left(\frac{1}{12r_0}(k_r + 6k_{rr} + 12k_\theta) + \frac{3\alpha_1}{8}SC_0\right)\left[\varepsilon_1^2 + \varepsilon_2^2 + \varepsilon_3^2\right] \\
&+ \left(\frac{\sqrt{3}}{12r_0}(k_r + 6k_{rr} - 6k_\theta) + \frac{3\sqrt{3}\alpha_2}{16}SC_0\right)\left[\varepsilon_1\varepsilon_2 + \varepsilon_1\varepsilon_3 + \varepsilon_2\varepsilon_3\right] \\
&+ \frac{1}{2}\left(\frac{\sqrt{3}}{12r_0}(k_r - 2k_{rr} + 4\sqrt{2}k_{r\theta} + 2k_\theta) + \frac{3\sqrt{3}\alpha_2}{16}SC_0\right)\left[\varepsilon_4^2 + \varepsilon_5^2 + \varepsilon_6^2\right] \\
&+ \left(\frac{1}{4r_0^2}(k_r - 2k_{rr} - 2\sqrt{2}k_{r\theta} - 4k_\theta) + \frac{9\alpha_4}{64r_0}SC_0\right)\left[u_x\varepsilon_1 + u_y\varepsilon_2 + u_z\varepsilon_3\right] \\
&+ \frac{1}{2}\left(\frac{\sqrt{3}}{4r_0^3}(k_r - 2k_{rr} - 8\sqrt{2}k_{r\theta} + 8k_\theta) + \frac{9\sqrt{3}\alpha_3}{128r_0^2}SC_0\right)\left[u_x^2 + u_y^2 + u_z^2\right].
\end{aligned}
\tag{11}
$$

Here we follow Martin [14] and employ the simplifying notation (in S.I. units) of S and C_0, where S is the dimensionless quantity, $\frac{Z^{*2}}{\epsilon_r}$, and C_0 has units of GPa and is given by: $\frac{e^2}{4\pi\epsilon_0 r_0^4}$. The quantities α_i are the numerical coefficients obtained by performing an Ewald summation at different strains, and adding to this the strain dependence of the linear repulsive term, which already contains within it the Madelung constant, α_M, which is an Ewald summation at zero strain. So for example, the result of performing an Ewald summation of these two electrostatic terms of the crystal for different strain states then yields an electrostatic energy which depends on strain as follows:

$$
\begin{aligned}
E_{el} &= \alpha_1\left(\varepsilon_1^2 + \varepsilon_2^2 + \varepsilon_3^2\right)SC_0 + \alpha_2(\varepsilon_1\varepsilon_2 + \varepsilon_1\varepsilon_3 + \varepsilon_2\varepsilon_3)SC_0 \\
&+ \frac{\alpha_2}{2}\left(\varepsilon_4^2 + \varepsilon_5^2 + \varepsilon_6^2\right)SC_0 + \alpha_3\left(\tilde{u}_x^2 + \tilde{u}_y^2 + \tilde{u}_z^2\right)SC_0 \\
&+ \alpha_4(\tilde{u}_x\varepsilon_4 + \tilde{u}_y\varepsilon_5 + \tilde{u}_z\varepsilon_6)SC_0.
\end{aligned}
\tag{12}
$$

Above we have utilized the notation $\tilde{u}_i = \frac{u_i}{a_0}$ so that the expansion coefficients all have the same units. We see reproduced above the result, expected from considerations of symmetry, that the coefficient of the electrostatic energy dependence on biaxial strain is double that of its dependence on shear strain [14,41,42]. The numerical values of these coefficients are given by:

$$
\begin{aligned}
\alpha_1 &= -0.128411, \quad \alpha_2 = -0.417608, \\
\alpha_3 &= -6.53970, \quad \alpha_4 = -3.62707.
\end{aligned}
\tag{13}
$$

When both the nearest neighbor terms and the Coulomb term have been so expanded in the strain, and the resulting energy density compared with Eq. (1), we may use Eqs. (9) to obtain the following expressions for our VFF force constants and effective charge:

$$
C_{11} = \frac{\sqrt{3}}{12r_0}(k_r + 6k_{rr} + 12k_\theta) + \frac{3\sqrt{3}\alpha_1}{8}SC_0,
$$

$$
C_{12} = \frac{\sqrt{3}}{12r_0}(k_r + 6k_{rr} - 6k_\theta) + \frac{3\sqrt{3}\alpha_2}{16}SC_0,
$$

$$
C_{44}^0 = \frac{\sqrt{3}}{3r_0}(k_r - 2k_{rr} + 4\sqrt{2}k_{r\theta} + 2k_\theta) + \frac{3\sqrt{3}\alpha_2}{16}SC_0,
$$

$$
D_{14} = \frac{1}{4r_0^2}(k_r - 2k_{rr} - 2\sqrt{2}k_{r\theta} - 4k_\theta) + \frac{9\alpha_4}{64r_0}SC_0,
$$

$$
E_{11} = \frac{\sqrt{3}}{4r_0^3}(k_r - 2k_{rr} - 8\sqrt{2}k_{r\theta} + 8k_\theta) + \frac{9\sqrt{3}\alpha_3}{128r_0^2}SC_0.
\tag{14}
$$

The expressions for the relaxed C_{44} and the Kleinman parameter ζ may be obtained from Eqs. (4) and (6).

In what follows, three different parametrizations of the VFF model are presented and discussed. Because there are many weakly-polar ZB and nonpolar diamond structured materials, and because the Coulomb interaction is the most computationally expensive to implement, in Sec. III A, we introduce a computationally efficient covalent VFF in which Coulomb terms are neglected. This parametrization is ideally suited to materials like C, Si, Ge or weakly polar III-V materials. However, as we will show it is not applicable to materials with ionicity and anisotropy past a certain threshold, such as, for example, InP and InAs. Therefore, in Sec. III B, the Coulomb potential is included via the conventional parametrization based on the optic mode splitting [14,42,43], and the effects of its inclusion on the stability of the model are discussed. It is found that this conventional parametrization results in a general increase in accuracy of the potential and restores stability for mildly ionic materials such as InP and InAs, but that this stabilizing effect is not sufficiently large for highly ionic and anisotropic materials such as cubic GaN and AlN. Thus, in Sec. III C a nonconventional inclusion of the Coulomb interaction is presented, whereby the effective charge is parametrized along with the force constants from the elastic energy density relations, ensuring stability with respect to any macroscopic or internal strain, and complete specification of the energy density of any diamond or ZB crystal.

All numerical quantities determined from the presented numerical relations in the following sections make use of the elastic and Kleinman parameters calculated in Ref. [39], while values for the zone-center optical phonon frequencies are taken from elsewhere in the literature and cited as used.

A. Covalent (non-Coulombic) VFF

To efficiently model nonpolar crystals, we may set S, in Eqs. (14), to 0. Then, using Eqs. (6) and (4), we obtain the following simplified expressions for C_{44} and ζ:

$$C_{44} = \frac{3\sqrt{3}}{2r_0} \frac{k_r k_\theta - 2k_{rr} k_\theta - 4k_{r\theta}^2}{k_r - 2k_{rr} - 8\sqrt{2}k_{r\theta} + 8k_\theta}, \tag{15}$$

$$\zeta = \frac{k_r - 2k_{rr} - 2\sqrt{2}k_{r\theta} - 4k_\theta}{k_r - 2k_{rr} - 8\sqrt{2}k_{r\theta} + 8k_\theta}. \tag{16}$$

We can invert these two equations, along with the expressions for C_{11} and C_{12} in Eq. (14). Taking care to eliminate the extraneous root that comes from a quadratic equation derived from C_{44} and ζ (see Appendix), we obtain direct expressions for the force constants in terms of the second order elastic constants and the Kleinman parameter. These read:

$$k_\theta = \frac{2(C_{11} - C_{12})r_0}{3\sqrt{3}}, \tag{17}$$

$$k_r = \frac{r_0[C_{11}(2 + 2\zeta + 5\zeta^2) + C_{12}(1 - 8\zeta - 2\zeta^2) + 3C_{44}(1 - 4\zeta)]}{\sqrt{3}(1 - \zeta)^2}, \tag{18}$$

$$k_{rr} = \frac{r_0[C_{11}(2 - 10\zeta - \zeta^2) + C_{12}(7 - 8\zeta + 10\zeta^2) - 3C_{44}(1 - 4\zeta)]}{6\sqrt{3}(1 - \zeta)^2}, \tag{19}$$

$$k_{r\theta} = \frac{r_0}{3}\sqrt{\frac{2}{3}} \frac{(C_{11} - C_{12})(1 + 2\zeta) - 3C_{44}}{\zeta - 1}. \tag{20}$$

Having this one-to-one analytic relation between the force constants and the elastic constants has several advantages. Like the Keating model we have direct expressions for the force constants with no numerical fitting procedures required. Thus, unlike potentials for which a numerical fitting is required, and a new fitting is needed for each material, Eqs. (17) to (20) ideally represent a VFF for any ZB or diamond structure material: Once the elastic constants and the Kleinman parameter are known, so too are the force constants. Unlike the Keating potential which describes exactly only the elastic constants C_{11} and C_{12}, with significant errors often found for C_{44} and ζ, the above relations ensure that these properties are reproduced exactly.

With respect to other more sophisticated potentials, this parametrization of the VFF model offers all the advantages of simplicity, efficiency, and clarity of the much used Keating model. The model even offers greater accuracy, in the regime for which it is parametrized, when compared to more complex potentials.

In addition, these simple expressions make the explanation of different trends in elastic properties in terms of the force constants a straightforward procedure. For example, Eqs. (14) and (17)–(20) may be used to obtain expressions for the other elastic constants, C_{44}^0, E_{11}, and D_{14}. These expressions may then be used to predict quantities on which the model has not been parametrized to ascertain the suitability of the potential for the different materials.

One such prediction is the value of the inner elastic constant E_{11}, which can be related to the experimental transverse optical phonon mode at the Γ point. While the potential is not aimed at the accurate description of dynamical properties, such quantities will nevertheless give an indication of whether or not the energetics of, for example, the internal strain, are reasonable. The quantity E_{11} is related to the frequency of the transverse optical phonon mode at Γ for ZB structures by Eq. (2). From Eqs. (14) and (17) to (20), the following relation

between E_{11} and the known elastic properties is derived:

$$E_{11} = \frac{16(C_{11} - C_{12} - C_{44})}{(1 - \zeta)^2 a_0^2}. \tag{21}$$

A negative E_{11} would lead to two undesirable results: imaginary ω_{TO} [cf Eq. (2)], and worse, the scenario that the energy density has a stationary point which is a maximum rather than a minimum in the internal strain; i.e., that the crystal is unstable with respect to internal strain. This latter consequence invalidates the basis of the whole procedure by which the relaxed elastic constants are derived, wherein the assumption is made that the energy is being *minimized* with respect to the internal strain.

An inspection of the terms in the numerator of Eq. (21) reveals that only those crystals for which $C_{11} - C_{12} > C_{44}$, or:

$$A = \frac{2C_{44}}{C_{11} - C_{12}} < 2, \tag{22}$$

where A is the anisotropy parameter [48], are stable against sublattice displacements. Furthermore, we note that this result is not restricted to our particular potential form but holds also for similar covalent potentials with Keating-style coordinates (i.e., a potential which is a function of dot products of bond vectors), and those with additional angle-angle coupling terms such as those in Refs. [11,16,42,49,50]. Thus, we may say that no nearest-neighbor VFF model can simultaneously describe C_{11}, C_{12}, C_{44}, and ζ for crystals with $A > 2$.

Relations of this kind may also be used in guiding numerical fittings away from dead ends with an appropriate choice of fitting weights. For example, Eq. (21) presents an upper limit on the accuracy with which the components of the elasticity of a ZB or diamond structured crystal can be simultaneously described using any nearest neighbor VFF model. The relation shows that, for example, in the work of Steiger *et al.* [42], if equal weights in the numerical fitting

TABLE I. Covalent VFF model prediction of E_{11} via Eq. (21), and zone-center transverse-optical phonon frequency, ω_{TO}, via Eq. (2). Experimental values and percentage differences between these and predicted values are given in brackets. a= Ref. [44]; b=Ref. [45]; c=Ref. [46]; d=Ref. [47].

	E_{11} (GPa Å^{-2})	ω_{TO} (cm^{-1})
AlN	-210.9	n/a
AlP	12.06	241 (454[a], -46%)
AlAs	11.09	209 (360[b], -42%)
AlSb	12.45	238 (318[c], -25%)
GaN	-132.9	n/a
GaP	22.45	269 (366[d], -27%)
GaAs	16.52	189 (273[d], -30%)
GaSb	13.40	173 (231[c], -25%)
InN	-282.0	n/a
InP	-2.62	n/a
InAs	-0.3	n/a
InSb	4.28	93 (185[c], -49%)

were given to C_{11}, C_{12}, C_{44}, E_{11}, and ζ, then it would not be possible to simultaneously minimize the residuals, and the fitting would go on forever.

The values of E_{11} predicted from Eq. (21), and the transverse optical phonon frequencies, ω_{TO}, corresponding to these are shown in Table I. Table I shows that, with negative predicted values for E_{11} and imaginary ω_{TO}, the potential is not suitable for the highly ionic cubic III-N or any of the indium containing III-Vs other than InSb. Simulations of these crystals with negative E_{11} using this potential are then unstable with respect to internal displacements.

Table I and the condition defined in Eq. (22) demonstrate that the VFF potential [Eq. (10)] parametrized via Eqs. (17)–(20), is suitable for neither the structural relaxation nor the dynamics of materials for which $A > 2$, while for materials with $A < 2$ the potential describes the parameters of the structural relaxation very well (C_{ij} and ζ), but does not accurately describe the Γ point optical phonons. These results have been further corroborated by actual structural relaxations, where materials with $A < 2$ relax to the correct equilibrium state and respond correctly to different applied strains. The force constants for selected III-V materials whose structural

TABLE II. Force constant values for the covalent VFF model for selected III-V semiconductors.

units	k_r eV Å^{-2}	k_θ eV rad^{-2}	k_{rr} eV Å^{-2}	$k_{r\theta}$ eV Å^{-1}rad^{-1}	S
AlP	5.505	0.401	0.640	0.453	0.000
AlAs	4.962	0.361	0.521	0.391	0.000
AlSb	4.557	0.294	0.320	0.249	0.000
GaP	6.237	0.464	0.455	0.421	0.000
GaAs	5.292	0.397	0.396	0.364	0.000
GaSb	4.542	0.319	0.264	0.258	0.000
InSb	3.194	0.218	0.362	0.248	0.000

relaxation is suitably described by the covalent VFF model are given in Table II.

From the fact that the inequality of Eq. (22) tends to be most strongly violated by the more ionic compounds, we can infer that the Coulomb interaction plays an important role in stabilizing heteropolar crystals, and that neglecting it is not justified. We therefore include the Coulomb interaction in the next subsection, using the conventional parametrization based on the splitting in zone-center transverse and longitudinal optical phonon mode frequencies.

B. Conventional inclusion of Coulomb interaction

Conventionally [14,42,43,51] the effective charge parameter, S, in a VFF potential is determined from the splitting between the optic mode frequencies at the Γ point. This relation is given in Eq. (23) below:

$$S = \frac{Z^{*2}}{\epsilon_r} = \left(\frac{\Omega}{4\pi e^2}\right)\mu\epsilon_0\left(\omega_{LO}^2 - \omega_{TO}^2\right). \quad (23)$$

Here Z^* is the effective charge, ϵ_r, in this relation, the high frequency dielectric constant of the material in question, Ω is the volume of the primitive cell, e is the electronic charge, ω_{LO} and ω_{TO} are the longitudinal and transverse optical phonon frequencies, respectively, and μ is the reduced mass of the anion and cation atoms. With this value for S, we may solve Eqs. (14) in a similar manner as before to obtain the following expressions for the force constants:

$$k_\theta = \frac{2\left(C_{11} - C_{12} + \frac{3\sqrt{3}}{8}(2\alpha_2 - \alpha_1)SC_0\right)r_0}{3\sqrt{3}}, \quad (24)$$

$$k_r = \frac{r_0[C_{11}(2 + 2\zeta + 5\zeta^2) + C_{12}(1 - 8\zeta - 2\zeta^2) + 3C_{44}(1 - 4\zeta) + SC_0(a_1 + a_2\zeta + a_3\zeta^2)]}{\sqrt{3}(1 - \zeta)^2}, \quad (25)$$

$$k_{rr} = \frac{r_0[C_{11}(2 - 10\zeta - \zeta^2) + C_{12}(7 - 8\zeta + 10\zeta^2) - 3C_{44}(1 - 4\zeta) + SC_0(a_4 + a_5\zeta + a_6\zeta^2)]}{6\sqrt{3}(1 - \zeta)^2}, \quad (26)$$

$$k_{r\theta} = \frac{r_0}{3}\sqrt{\frac{2}{3}}\frac{(C_{11} - C_{12})(1 + 2\zeta) - 3C_{44} + SC_0(a_7 + a_8\zeta)}{\zeta - 1}. \quad (27)$$

TABLE III. Force constant values for selected III-V semiconductors using the Coulombic VFF model fitted to optical phonon frequency splitting.

	k_r	k_θ	k_{rr}	$k_{r\theta}$	S
units	eV Å^{-2}	eV rad^{-2}	eV Å^{-2}	eV Å^{-1}rad^{-1}	
AlP	7.017	0.392	0.450	0.333	0.689
AlAs	6.880	0.349	0.279	0.240	0.593
AlSb	5.550	0.289	0.192	0.173	0.373
GaP	7.841	0.453	0.263	0.287	0.510
GaAs	6.520	0.389	0.250	0.261	0.448
GaSb	5.068	0.315	0.199	0.215	0.222
InN	10.513	0.272	0.862	0.425	1.996
InP	5.892	0.276	0.366	0.262	0.609
InAs	5.031	0.243	0.325	0.227	0.551
InSb	4.272	0.213	0.215	0.172	0.384

Here the a_i denote combinations of Ewald summation terms:

$$a_1 = -\frac{12\sqrt{3}}{128}(8\alpha_1 + 8\alpha_2 + 3\alpha_4),$$

$$a_2 = -\frac{6\sqrt{3}}{128}(16\alpha_1 - 80\alpha_2 - 3\alpha_3),$$

$$a_3 = -\frac{3\sqrt{3}}{128}(80\alpha_1 - 16\alpha_2 - 3\alpha_3 + 24\alpha_4),$$

$$a_4 = \frac{12\sqrt{3}}{128}(-8\alpha_1 - 8\alpha_2 + 3\alpha_4),$$

$$a_5 = \frac{6\sqrt{3}}{128}(80\alpha_1 - 16\alpha_2 - 3\alpha_3),$$

$$a_6 = \frac{3\sqrt{3}}{128}(16\alpha_1 - 80\alpha_2 - 3\alpha_3 + 24\alpha_4),$$

$$a_7 = -\frac{6\sqrt{3}}{128}(8\alpha_1 - 16\alpha_2 + 3\alpha_4),$$

$$a_8 = -\frac{3\sqrt{3}}{128}(32\alpha_1 - 16\alpha_2 - 3\alpha_3 + 6\alpha_4).$$

Note that Eqs. (24)–(27) are identical to the covalent equations [Eqs. (17)–(20)] apart from the electrostatic addition; the non-Coulombic case can be recovered by setting $S = 0$. Force constants and effective charge parameters for selected III-V materials obtained from Eqs. (24)–(27) are given in Table III.

Using these new force constant expressions, the inner elastic constant, E_{11}, predicted by the model is given by the relation:

$$E_{11} = \frac{16(C_{11} - C_{12} - C_{44} + 0.135645\,C_0 S)}{(1 - \zeta)^2 a_0^2}, \quad (28)$$

where the numerical factor 0.135645 results from the sum: $\frac{3\sqrt{3}}{8}(-\alpha_1 + \alpha_2 + \frac{\alpha_3}{16} - \frac{\alpha_4}{4})$. From this equation the stabilizing effect of the Coulomb interaction is apparent: The larger the product SC_0, the less strict need be the inequality $C_{11} - C_{12} > C_{44}$ to maintain stability. Thus, materials with an anisotropy parameter $A > 2$, which are unstable in the purely covalent model, can be stabilized by the inclusion of Coulomb effects. Table IV illustrates this for the parametrization used here, where the calculated value of E_{11} is given for the III-V materials that we consider.

Table IV shows that while many materials unstable in the non-Coulombic case have become stable, the Coulomb interaction derived from Eq. (23) is not sufficient to stabilize the highly ionic cubic III-N materials AlN and GaN. Furthermore, we note that while InN is stable while utilizing the optical phonon splitting of Kim *et al.* [43], using other results (e.g., from Ref. [61]) for ω_{TO} and ω_{LO} will yield a smaller value for S and an unstable crystal.

Nevertheless, the values of ω_{TO} derived using Eq. (2) and presented in Table IV reveal a universal reduction in

TABLE IV. Properties relevant to, and predicted from, the conventionally parametrized Coulombic VFF. First four columns are related to Eq. (28) and the predicted value of the internal elastic constant, E_{11}. $C' = C_{11} - C_{12}$, and C_{44} are obtained from Ref. [39], S is determined using Eq. (23) with experimental phonon frequencies, and C_0 is the quantity $\frac{e^2}{4\pi\epsilon_0 r_0^4}$. The ω_{TO} and ω_{LO} columns compare VFF-predicted phonon frequencies with experiment and the Z^* column gives effective charges obtained from experiment via Eq. (23), using values for ε_r from Ref. [52], and gives in brackets, where available, *ab initio* values. Superscripts a–k indicate where experimental values of ω_{TO} and ω_{LO}, or theoretical values of Z^*, were obtained: a=Ref. [43]; b=Ref. [44]; c=Ref. [45]; d=Ref. [47]; e=Ref. [53]; f=Ref. [54]; g=Ref. [55]; h=Ref. [52]; i=Ref. [56]; j=Ref. [57]; k=Ref. [58]; l=Ref. [53]; m=Ref. [59]; n=Ref. [60].

	$C'-C_{44}$ (GPa)	S	$0.136\,C_0S$ (GPa)	E_{11} (GPa Å^{-2})	ω_{TO} (cm^{-1})	ω_{LO} (cm^{-1})	Z^*
AlN	−53.48	1.5454[a]	37.91	−61.40	n/a	n/a	2.73 (2.70[j])
AlP	4.00	0.6888[b]	6.84	32.22	342 (454[b],25%)	390 (491[b],21%)	2.28 (−)
AlAs	4.06	0.5931[c]	5.05	24.91	313 (360[c],13%)	361 (402[c],10%)	2.21 (2.17[k])
AlSb	5.03	0.3728[d]	2.26	18.07	287 (323[d],11%)	310 (344[d],10%)	1.95 (1.91[k])
GaN	−31.31	1.3373[e]	29.23	−8.83	n/a	n/a	2.55 (2.65[l])
GaP	9.11	0.5098[d]	5.11	35.03	336 (366[d],8 %)	376 (403[d],7 %)	2.16 (2.03[m])
GaAs	7.41	0.4476[d]	3.81	25.01	232 (273[d],15%)	259 (296[d],13%)	2.20 (2.19[n])
GaSb	6.38	0.2224[f]	1.38	16.33	191 (231[f],17%)	202 (240[f],16%)	1.79 (1.73[k])
InN	−28.01	1.9960[g]	28.64	6.37	164 (478[g],66%)	529 (694[g],24%)	4.09 (3.02[j])
InP	−0.69	0.609[h]	5.08	14.29	226 (307[h],26%)	294 (343[h],14%)	2.58 (2.38[m])
InAs	−0.10	0.5507[i]	3.50	11.10	154 (217[i],29%)	185 (240[i],23%)	2.61 (−)
InSb	1.55	0.3839[i]	1.84	9.54	139 (180[i],23%)	155 (192[i],20%)	2.45 (−)

the error, when compared with the non-Coulombic results presented in Table I. Furthermore, with the addition of the Coulomb interaction, the qualitative description of the zone-center optical phonons is greatly improved, with ω_{TO} and ω_{LO} no longer degenerate. The values of ω_{TO} and ω_{LO} predicted using the VFF described by Eqs. (23) and (24)–(26) are given in Table IV. In addition, we see from Table IV that the effective charge parameter S, obtained from experiment via Eq. (23), produces Born effective charges, Z^*, which are in good agreement with those determined from first-principles calculations.

However, given our aim is to completely describe the elastic energy of any ZB or diamond structure material, the instabilities found for AlN and GaN lead to the conclusion that for this VFF model, the conventional Coulomb parametrization is not appropriate when modeling highly ionic materials. Other approaches to the parametrization of the effective charge exist in the literature: For example, Grosse and Neugebauer [51] used the difference in the total energies of ZB and wurtzite phases of the III-N materials, AlN, GaN, and InN to determine the effective charge, and Barret and Wang [62] introduced a model where the atomic charge is separated from the Born effective charge, and both are utilized in a double charge model for the accurate treatment of the lattice dynamics of surfaces. However, in both of these methods, the charge parameter S produced is smaller than that obtained using Eq. (23).

Therefore, in the next section, we seek a more direct means of ensuring that the VFF model correctly describes the dependence of the energy of the crystal on the internal strain. This involves breaking with the conventional parametrization of the effective charge, and setting the parameter S such that the inner elastic constant E_{11} is exactly reproduced. With this parametrization, the elastic energy density and internal strain of a ZB or diamond crystal will then be well described by the VFF for any combination of macroscopic and internal strain.

C. Inner elastic parametrization of effective charge

In order to guarantee that the elastic energy density is completely described by our VFF model we include the inner elastic constant E_{11} in the fitting and solve for S such that the correct, positive value is reproduced. Thus the interaction parameters k_r, k_θ, k_{rr}, $k_{r\theta}$, and S are obtained from the known elastic constants C_{11}, C_{12}, C_{44}, ζ, and E_{11}. This ensures not only that the crystal will be stable against shear and internal strains, since we are fitting directly to a positive E_{11}, but also that the dependence of the free energy of any diamond or ZB crystal on any combination of macroscopic and internal strain, will be described completely. Allowing S to be set in this way is justified because there is in any case some degree of arbitrariness in the choice of the *effective* charge, given delocalization and screening effects present in the crystal.

To achieve this parametrization we make use of Eq. (28), which gives the value of E_{11} in terms of C_{11}, C_{12}, C_{44}, ζ, and S. We now solve this equation for S, to obtain the following expression:

$$S = \frac{E_{11}(1-\zeta)^2 a_0^2 - 16(C_{11} - C_{12} - C_{44})}{6\sqrt{3}C_0(-\alpha_1 + \alpha_2 + \alpha_3/16 - \alpha_4/4)}. \quad (29)$$

TABLE V. Force constant values determined using the Coulombic VFF model with effective charges determined by elastic and inner elastic properties.

units	k_r eV Å^{-2}	k_θ eV rad^{-2}	k_{rr} eV Å^{-2}	$k_{r\theta}$ eV Å^{-1}rad^{-1}	S
AlN	23.52	0.506	−0.024	0.517	3.378
AlP	9.30	0.379	0.162	0.361	1.046
AlAs	8.00	0.343	0.139	0.371	0.9387
AlSb	6.42	0.284	0.081	0.283	0.6991
GaN	19.17	0.536	0.239	0.696	2.45786
GaP	8.67	0.447	0.165	0.514	0.7721
GaAs	7.90	0.379	0.087	0.357	0.9490
GaSb	6.43	0.307	0.032	0.275	0.8052
InN	14.75	0.263	0.220	0.467	2.3266
InP	7.71	0.269	0.115	0.356	1.04947
InAs	6.85	0.235	0.077	0.264	1.0794
InSb	5.49	0.208	0.049	0.246	0.8252

Substituting the value for S thus obtained into Eqs. (24)–(27) yields the required potential.

With this potential, all elastic properties input are reproduced exactly, as is ω_{TO}, through the inner elastic constant E_{11}. The force constants obtained using Eqs. (29) and (24)–(27), for selected III-V materials, are shown in Table V. Of particular note in Table V is the much larger screened Coulomb parameter $S = \frac{Z^{*2}}{\epsilon_r}$ compared to the conventional parametrization shown in Table III. We attribute this to the greater importance of short-ranged Coulomb interactions over long-ranged interactions for the stabilization of the crystal with respect to internal strains. Interactions between closer atoms will have fewer atoms and electrons between them to screen the field, and prioritizing these interactions will manifest as a larger S in the potential. In addition, it is possible that longer range forces other than the Coulomb interaction are being effectively incorporated into this parameter. Either way, the potential represents a significant improvement in the description of the elastic properties of the highly ionic ZB structured materials.

Table VI shows a comparison of calculated ω_{LO} versus previous theory and experimental values. Comparing with Table IV, we find that the inner elastic parametrization offers a universal improvement over the conventional parametrization. Being directly fitted to E_{11} it reproduces ω_{TO} exactly, and for ω_{LO}, to which it was not fit, it also performs considerably better.

In the next section, we will perform a further benchmarking of each of the potentials. We first benchmark the models against first principles DFT relaxations. We find the agreement between the VFF relaxed atomic positions and those obtained from DFT is good, and that again, the new effective charge parametrization produces the best results. We then compare their relative performances in the calculation of phonon spectra, where we show best overall agreement with experiment is again obtained for the third model presented.

TABLE VI. Value of transverse and longitudinal optical phonon frequency at the Γ point, ω_{LO}, predicted from Coulombic VFF potential with effective charges determined by elastic and inner elastic properties. Experimental values and percentage difference are given in brackets. Apart from AlN, a=Ref. [43], and GaN, b=Ref. [53], all experimental values are the same as those in Table IV.

	ω_{TO} (cm^{-1})	ω_{LO} (cm^{-1})
AlN	654 (654[a],0%)	1145(908[a],−26%)
AlP	454 (454,0%)	542 (491, −10%)
AlAs	360 (360,0%)	425 (402, −6%)
AlSb	323 (323,0%)	362 (344, −5%)
GaN	560 (560[b],0%)	878 (750[b],−17%)
GaP	366 (366,0 %)	421 (403, −4%)
GaAs	273 (273,0%)	321 (296, −8%)
GaSb	231 (231,0%)	262 (240,−9%)
InN	478 (478,0%)	724 (694, −4%)
InP	307 (307,0%)	369 (350, −6%)
InAs	217 (217,0%)	260 (240, −8%)
InSb	180 (180,0%)	203 (192, −6%)

IV. COMPARISON WITH EXPERIMENTAL AND *ab initio* DATA

In this section, we present a benchmarking of the three different potentials. We first validate the potentials for use as a tool for structural relaxation: We find, using each potential, the relaxed atomic positions in various InAs/GaAs supercells and compare these positions with those obtained from DFT calculations within the local density approximation (LDA). Then, we analyze and compare with experiment the VFF calculated phonon band structure of GaAs. Our choice of GaAs/InAs systems for benchmarking is based on the following considerations: InAs/GaAs heterostructures are one of the most technologically relevant semiconductor material systems, widely studied, and grown along various different crystallographic directions [27]; secondly, both InAs and GaAs are ionic materials, with InAs being a material for which the anisotropy factor is just past the threshold of stability ($A < 2$) for the covalent potential, and therefore a system which is a combination of these two binary compounds serves as an ideal test bed for the different variants of the potential.

To benchmark the potentials against first principles structural relaxations, we first parametrize our VFF using elastic constants from DFT calculations commensurate with those from which the relaxed atomic positions were determined. While the force constants presented earlier will more accurately reproduce the true atomic positions (since the hybrid-functional-DFT elastic constants agree better with experiment), performing test structure relaxations using HSE DFT is computationally costly and not necessary. When benchmarking, no extra information is gained by making comparisons to a computationally more expensive functional.

The elastic constants C_{ij} and the Kleinman parameter ζ were calculated using LDA DFT, as implemented in the VASP code [63], using a k-point grid of $16 \times 16 \times 16$ and a cutoff energy of 600 eV, and are given in Table VII. These elastic constants were used to parametrize the three VFF models via Eqs. (17) to (20), Eqs. (24) to (27), and (23) and (29).

Next, four different supercells have been relaxed using LDA DFT: (i) a simple GaAs/InAs interface along the [001] crystallographic direction, modelled as a supercell of alternating GaAs/InAs conventional unit cells, containing 16 atoms and having unrelaxed dimensions $a_0, a_0, 2a_0$, where $a_0 = 5.6198$ Å, in the x, y, and z directions, respectively; (ii) a (001) quantum well type interface, consisting of a GaAs cubic unit cell, an InAs cubic unit cell, and then another GaAs cell, containing 24 atoms and having initial dimensions $a_0, a_0, 3a_0$; (iii) a GaAs/InAs interface along the [111] direction, consisting of alternating GaAs/InAs six-atom unit cells [32,64] with the z axis along the [111] direction, containing 12 atoms and having unrelaxed lattice vectors $a_1 = (\frac{a_0}{\sqrt{2}}, 0, 0)$, $a_2 = (\frac{a_0}{2\sqrt{2}}, \frac{\sqrt{3}a_0}{2\sqrt{2}}, 0)$, $a_3 = (0, 0, 2\sqrt{3}a_0)$; (iv) a 64 atom GaInAs supercell, consisting of a $2 \times 2 \times 2$ replication of a conventional ZB cell, with In atoms substituted for Ga atoms with a probability according to the nominal In content of 25%. For each of these supercells, the total free energy was minimized until the force on any atom was less than 0.001 eV/Å. The LDA calculations were in all cases performed with a cutoff energy of 600 eV, and k-point grid densities of: $12 \times 12 \times 6$, $12 \times 12 \times 4$, $12 \times 12 \times 5$, and $8 \times 8 \times 8$, for supercells (i)–(iv), respectively.

Following the relaxation of each of these supercells using LDA DFT, the same supercells were relaxed using the three parametrizations of the VFF in the software package GULP [23]. A summary of the comparison between the relaxations produced by these VFF potentials and LDA DFT is presented in Table VIII.

Examining first the averaged results presented at the bottom of Table VIII, a trend of increasing accuracy in the reproduction of all quantities is seen when progressing from the covalent potential, through to the conventionally parametrized ionic potential, to the new inner elastic parametrization of the effective charge. This suggests the importance of accurately describing E_{11} for structural relaxations.

Looking in more detail, we find for the covalent potential that it is able to well relax the two [001] oriented systems for which there are no macroscopic shear strains, but it fails completely for the (111) interface and alloy systems. For the [111]-oriented system, GULP is unable to minimize the energy density resulting from the unstable potential. For the alloy supercell GULP is able to achieve a minimum, owing to the stabilizing effect of the GaAs matrix, but the instability of the InAs VFF with respect to shear strains is manifested in larger errors in bond lengths and angles. For the ionic potentials, a good description of the lattice and bond properties is found for all systems, and unlike the covalent potentials, there

TABLE VII. LDA DFT calculated elastic and structural properties of GaAs and InAs. Calculations were performed on a k-point grid of $16 \times 16 \times 16$ and a plane-wave cutoff energy of 600 eV. a_0 is in Å, C_{ij} are in GPa, ζ is dimensionless, and E_{11} is in GPa Å^{-2}.

	a_0	C_{11}	C_{12}	C_{44}	ζ	E_{11}
GaAs	5.6198	115	52	58	0.547	34
InAs	6.0312	85	48	38	0.687	23

TABLE VIII. Percentage differences between structural properties of supercells relaxed using LDA DFT, and three different VFF models. See text for description of supercells; 'All' refers to an averaging of all supercell errors. VFF (a) is the covalent VFF, (b) is the conventional Coulombic VFF, and (c) is the elastically parametrized Coulombic VFF. $\overline{\Delta|\mathbf{a}_i|}$ denotes the average difference in the magnitude of the lattice vectors, $\overline{\Delta r_{ij}}$ is the average difference in all bond lengths, and $\overline{\Delta\theta}$ is the average difference in angles.

Supercell	VFF	$\overline{\Delta|\mathbf{a}_i|}(\%)$	$\overline{\Delta r_{ij}}\ (\%)$	$\overline{\Delta\theta}(\%)$
	(a)	0.45	0.15	0.33
[001] GaAs/InAs	(b)	0.35	0.27	0.32
	(c)	0.36	0.15	0.26
	(a)	0.36	0.07	0.27
[001] GaAs/InAs/GaAs	(b)	0.28	0.19	0.27
	(c)	0.26	0.11	0.22
	(a)			
[111] GaAs/InAs	(b)	0.19	0.37	0.48
	(c)	0.22	0.32	0.48
	(a)	0.03	1.94	1.5
InGaAs alloy	(b)	0.04	0.35	0.37
	(c)	0.05	0.25	0.32
	(a)	0.28	0.72	0.70
All	(b)	0.22	0.30	0.36
	(c)	0.22	0.21	0.32

is no increase in the errors for the [111]-oriented or alloyed structures. For all potentials, aside from the unstable covalent potential, the errors in the relaxation of the alloy supercell are much lower than those in the layered systems. This may be imputed to nonlinear strain effects experienced in the sharply interfaced supercells—the errors in this case could be reduced by inclusion of anharmonic force constants and third order elastic constants [39]. Overall, the agreement between the first-principles and VFF relaxations of the here-considered supercells is very good and serves to validate the VFF for use in larger scale structural relaxations.

Next, the full phonon band structure of GaAs, calculated using each parametrization of the potential, and determined experimentally [65], is shown in Fig. 3. All three of the parametrizations share a good description of the acoustic modes, near the Γ point especially, with the description of the longitudinal acoustic modes remaining good at larger wave vectors. All three potentials share the property that the softening of the transverse acoustic mode, in the Γ to X, L, and K directions, is not well described; this is a characteristic feature of nearest neighbor VFFs, and may be remedied, for example, by inclusion of an angular interaction term which involves four coplanar bonds [10,42,62,66,67]. However, given that our aim is to introduce a potential for simple, accurate, and efficient structural relaxation, rather than accurate phonon dispersions through the full Brillouin zone, we do not here include this term.

Looking to the differences between the different potentials, we find that, compared to the other two, the covalent VFF has larger errors in the longitudinal acoustic modes at large wave vectors and that its description of the optical modes is qualitatively and quantitatively significantly inferior to that
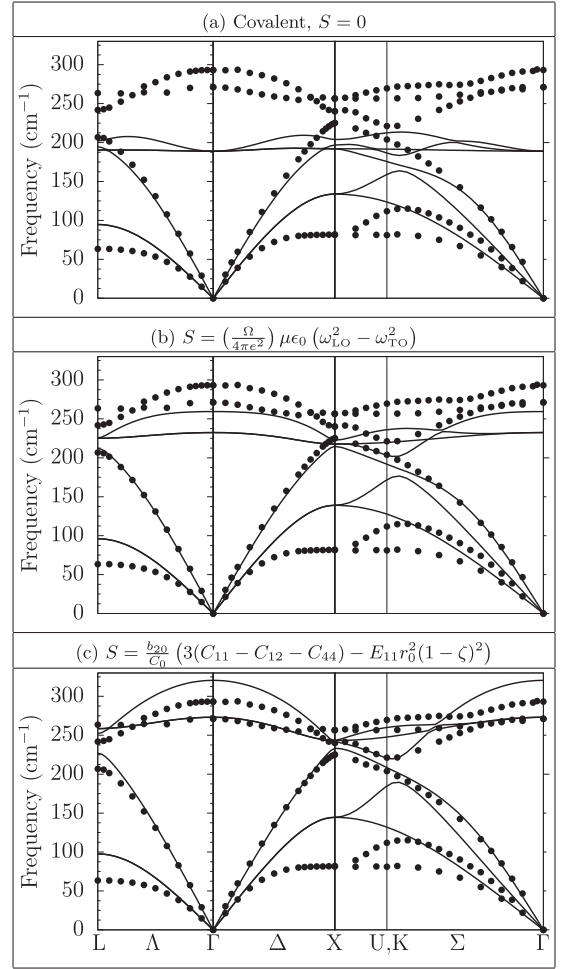

FIG. 3. Phonon band structure of GaAs calculated using different VFF parametrizations: (a) band structure calculated using covalent VFF with effective charge parameter $S = 0$, and force constants described by Eqs. (17)–(20); (b) band structure calculated using ionic VFF, with effective charge determined via Eq. (23), and force constants determined by Eqs. (24)–(27); (c) band structure calculated using ionic VFF, with effective charges determined via Eq. (29) and force constants given by Eqs. (24)–(27). The filled symbols are experimental frequencies taken from Ref. [65].

of the two ionic potentials; this is to be expected, given the non-negligible ionicity of GaAs. Comparing the two ionic models, we find that using E_{11} to parametrize the effective charge produces a band structure which generally agrees better with experiment than that produced by the potential with a conventionally parametrized effective charge; however, the conventional parametrization does produce better agreement with experiment for the longitudinal acoustic branch at L.

Overall, we can conclude that all potentials reproduce well the acoustic branches near the Γ point, while the best agreement with experiment throughout the Brillouin zone is obtained by the potential in which the effective charge is determined by fitting to the elastic and inner elastic properties. This shows, in combination with Table VIII, that the new Coulombic parametrization produces improved relaxation *and* phonon spectra compared to the conventional parametrization.

V. CONCLUSION

In conclusion, we have presented a VFF model, based on that originally introduced by Musgrave and Pople [11] and modified by Martin [14], which explicitly fits to the often neglected and ill-described Kleinman parameter, as well as the three cubic second order elastic constants, of which C_{44} is often poorly represented in the popular Keating model [5]. Three different parametrizations of the potential were presented: a covalent (non-Coulombic) one for nonionic or weakly ionic materials; and two parametrizations which include electrostatic forces, in one of which we determine the effective charges via zone-center phonon frequency splittings, while in the second case the effective charges are determined via the inner elastic properties.

The force constants of the model were derived analytically with explicit expressions given for them in terms of macroscopic elastic constants, as well as inner elastic properties which can be measured and/or directly calculated using density functional theory. This allows the potential to be used for a given material without the need for any additional numerical fitting: Once the elastic and related properties of the material are known, the force constants can be obtained immediately from them by means of the analytic expressions presented here.

In addition to ease of application, the analytic determination of force constants also has the advantage that it allows for the *a priori* prediction of properties outside of the determining parameter set of the potential. This capability allowed for the analysis of the suitability of the potential for application to different materials. This analysis furnished the result (general for nearest neighbor VFFs), that a stable non-Coulombic potential which accurately describes the three cubic elastic constants and Kleinman's internal strain parameter is not achievable for materials for which the anisotropy factor, A, is >2. The stabilizing effect of the Coulomb interaction was first examined based on conventional parametrization in terms of the optical phonon splitting frequency. This parametrization was found to stabilize most materials, with the exception of the highly ionic cubic III-N materials, GaN and AlN. This instability was remedied by use of a new parametrization of the effective charges, which resulted in a potential capable of fully describing the elastic energy density of any diamond or zincblende crystal. In benchmarking against density functional theory and experiment, this new parametrization of the effective charge was shown to produce improved phonon spectra and structural relaxations.

The described potential thus offers an efficient, intuitive, and accurate description of all classes of zincblende or diamond crystal, with increased accuracy, efficiency, and clarity when compared with machine-learning-based or other complex potentials, and with increased accuracy at little extra computational cost when compared with the extensively used simpler VFFs often used for structural relaxation in the literature.

APPENDIX

We note that Eqs. (14) provide five linear relationships between five macroscopic elastic constants (C_{11}, C_{12}, C_{44}^0, D_{14}, and E_{11}) and the five parameters required in our general VFF model. We can therefore solve these linear equations directly to obtain expressions for the VFF parameters in terms of macroscopic elastic properties that can be determined using well established DFT approaches. While this is useful, it may be generally preferred to calculate the VFF parameters in terms of the experimentally accessible elastic constants, C_{11}, C_{12}, and C_{44}, as well as the internal strain parameter ζ, in particular given that an accurate description of ζ is required for an accurate description of relative atomic displacements within a given unit cell. We outline here how the covalent VFF terms can be calculated from the linear expressions for C_{11} and C_{12} in Eqs. (14) and from the nonlinear expressions for C_{44} and ζ in Eqs. (15) and (16). The method that we describe can be readily modified to treat the more general case of the ionic potential with additional terms proportional to SC_0.

Subtracting C_{11} from C_{12} in Eqs. (14) reveals immediately the unique determination of k_θ in terms of C_{11} and C_{12}:

$$k_\theta = \frac{2r_0}{3\sqrt{3}}(C_{11} - C_{12}). \tag{A1}$$

Adding twice C_{12} to C_{11} in Eqs. (14) furnishes a linear expression for k_{rr} in terms of C_{11}, C_{12}, and k_r:

$$k_{rr} = \frac{2r_0}{3\sqrt{3}}(C_{11} + 2C_{12}) - \frac{k_r}{6}. \tag{A2}$$

Multiplying out Eq. (16) and utilising Eq. (A2), a linear expression relating $k_{r\theta}$ to k_r is obtained:

$$k_r = k_{r\theta}\frac{3}{\sqrt{2}}\frac{4\zeta - 1}{\zeta - 1} - \frac{3k_\theta(2\zeta + 1)}{\zeta - 1} + \frac{r_0(C_{11} + 2C_{12})}{\sqrt{2}}. \tag{A3}$$

Having now expressions for k_{rr} in terms of k_r, and $k_{r\theta}$ in terms of k_r, the remaining equation for C_{44}, Eq. (6), can be cast in terms of only $k_{r\theta}$ and known elastic constants. Expanding out Eq. (6) we are left with the quadratic equation:

$$\overbrace{\frac{3}{2r_0^2}}^{a} k_{r\theta}^2 + \overbrace{\frac{3C_{44} + C'(1 - 4\zeta)}{\sqrt{6}(\zeta - 1)r_0}}^{b} k_{r\theta}$$
$$+ \underbrace{\frac{C'(C' - 3C_{44} + 2C'\zeta)}{9(\zeta - 1)}}_{c} = 0. \tag{A4}$$

This may be solved using the quadratic formula: $k_{r\theta} = \frac{-b \pm \sqrt{b^2 - 4ac}}{2a}$. The two solutions then correspond to different values of $k_{r\theta}$, k_{rr}, and k_r, with the same k_θ. However, implementation of this formula reveals one of the solutions to be extraneous, as discussed further below.

Taking the coefficients from Eq. (A4), we obtain:

$$b^2 - 4ac = \frac{3}{2r_0^2} \frac{(C_{44} - C')^2}{(\zeta - 1)^2}. \tag{A5}$$

Putting this into the quadratic formula and simplifying, we obtain:

$$k_{r\theta} = -\frac{4r_0}{3\sqrt{6}} \frac{3C_{44} - C'(1 - 4\zeta)}{\zeta - 1} \pm \frac{4r_0^2}{3} \sqrt{\frac{3}{2}\left(\frac{C_{44} - C'}{(\zeta - 1)r_0}\right)^2}. \tag{A6}$$

These two solutions simplify to:

$$k_{r\theta}^+ = \frac{2}{3}\sqrt{\frac{2}{3}} r_0 C' = \sqrt{2}k_\theta, \tag{A7}$$

and, already given in Eq. (20) in Sec. III A above:

$$k_{r\theta}^- = \frac{r_0}{3}\sqrt{\frac{2}{3}} \frac{(C_{11} - C_{12})(1 + 2\zeta) - 3C_{44}}{\zeta - 1}. \tag{A8}$$

By inspection of Eq. (14) we can see that the extraneous solution is that in Eq. (A7), which would lead to the undefined scenario of 0/0 in Eqs. (15) and (16). Furthermore,

we see that whether this solution is that with the positive or negative root depends on whether $C_{44} > C'$, equivalent to whether $A > 2$. In addition, we note that these two conditions also govern whether or not the VFF will be stable against internal strain ($E_{11} > 0$); so the result also holds that as the sign of the extraneous solution changes, so does the sign of E_{11}. When this sign change occurs, the underlying assumption in the derivation of the equations that the energy has been minimized with respect to the internal strain becomes invalid.

Thus, the single correct analytic expression for the force constant $k_{r\theta}$ in terms of the elastic constants and the Kleinman parameter is the right hand solution in Eq. (A8). Via Eqs. (A1), (A2), and (A3), we then obtain the full single set of force constants of Eqs. (17)–(20).

Alternatively, the pitfalls of the extraneous root may be more efficiently circumvented by simply solving the equation set comprising C_{11}, C_{12}, and ζ, from Eq. (14) along with the rightmost expression of Eq. (6), where the ζ is not swopped for its numerical value, but rather left as a known numerical quantity. Choosing this set of equations a quadratic term in $k_{r\theta}$ never arises, and there is simply a squared ζ, which adds no extra roots to the equation set.

---

[1] A.-J.-C. B. de St. Venant, Mémoires des Savants étrangers **14**, 233 (1855).

[2] M. Born and K. Huang, *Dynamical Theory of Crystal Lattices*, Oxford Classic Texts in the Physical Sciences (Clarendon Press, Oxford, 1954).

[3] A. Thompson, L. Swiler, C. Trott, S. Foiles, and G. Tucker, J. Comput. Phys. **285**, 316 (2015).

[4] A. P. Bartók, M. C. Payne, R. Kondor, and G. Csányi, Phys. Rev. Lett. **104**, 136403 (2010).

[5] P. N. Keating, Phys. Rev. **145**, 637 (1966).

[6] C. S. G. Cousins, J. Phys. C **11**, 4867 (1978).

[7] C. S. G. Cousins, J. Phys. C **15**, 1857 (1982).

[8] C. Feldman, M. L. Klein, and G. K. Horton, Phys. Rev. **184**, 910 (1969).

[9] S. W. Ellaway and D. A. Faux, J. Appl. Phys. **92**, 3027 (2002).

[10] C. S. G. Cousins, Phys. Rev. B **67**, 024107 (2003).

[11] M. J. P. Musgrave and J. A. Pople, Proc. R. Soc. London A **268**, 474 (1962).

[12] H. McMurry, A. Solbrig, and J. Boyter, J. Phys. Chem. Solids **28**, 2359 (1967).

[13] M. A. Nusimovici and J. L. Birman, Phys. Rev. **156**, 925 (1967).

[14] R. M. Martin, Phys. Rev. B **1**, 4005 (1970).

[15] M. Z. Bazant, Interatomic forces in covalent solids, Ph.D. thesis, Harvard University, 1997.

[16] D. Vanderbilt, S. H. Taole, and S. Narasimhan, Phys. Rev. B **40**, 5657 (1989).

[17] M. Łopuszyński and J. A. Majewski, J. Phys.: Condens. Matter **22**, 205801 (2010).

[18] C. S. Schnohr, J. Phys.: Condens. Matter **24**, 325802 (2012).

[19] E. P. O'Reilly, Semicond. Sci. Technol. **4**, 121 (1989).

[20] C. Pryor, J. Kim, L. W. Wang, A. J. Williamson, and A. Zunger, J. Appl. Phys. **83**, 2548 (1998).

[21] G. Bester and A. Zunger, Phys. Rev. B **71**, 045318 (2005).

[22] S. J. Plimpton, J. Comput. Phys. **117**, 1 (1995).

[23] J. D. Gale, A. L. Rohl, and D. C. Hibbens-Butler, Mol. Simul. **29**, 291 (2003).

[24] E. Nielsen, R. Rahman, and R. P. Muller, J. Appl. Phys. **112**, 114304 (2012).

[25] M. Zieliński, Phys. Rev. B **86**, 115424 (2012).

[26] M. Zieliński, J. Phys.: Condens. Matter **25**, 465301 (2013).

[27] R. Benchamekh, S. Schulz, and E. P. O'Reilly, Phys. Rev. B **94**, 125308 (2016).

[28] C. S. G. Cousins, Inner Elasticity and the higher-order elasticity of some diamond and graphite allotropes, Ph.D. thesis, University of Exeter, 2001.

[29] W. Voigt, *Lehrbuch der Kristallphysik* (Teubner, Leipzig, 1928).

[30] J. F. Nye, *Physical Properties of Crystals: Their Representation by Tensors and Matrices*, 2nd ed. (Oxford University Press, Oxford, 1985).

[31] O. H. Nielsen and R. M. Martin, Phys. Rev. B **32**, 3792 (1985).

[32] M. A. Caro, S. Schulz, and E. P. O'Reilly, J. Phys.: Condens. Matter **25**, 025803 (2013).

[33] L. Kleinman, Phys. Rev. **128**, 2614 (1962).

[34] C. S. G. Cousins, L. Gerward, J. S. Olsen, B. Selsmark, and B. J. Sheldon, J. Phys. C **20**, 29 (1987).

[35] C. S. G. Cousins, L. Gerward, J. S. Olsen, B. Selsmark, B. J. Sheldon, and G. E. Webster, Semicond. Sci. Technol. **4**, 333 (1989).

[36] C. S. G. Cousins, L. Gerward, J. S. Olsen, and B. J. Sheldon, J. Phys.: Condens. Matter **1**, 4511 (1989).

[37] C. S. G. Cousins, L. Gerward, J. S. Olsen, S. A. Sethi, and B. J. Sheldon, Phys. Status Solidi (a) **126**, 135 (1991).

[38] M. A. Caro, S. Schulz, and E. P. O'Reilly, Phys. Rev. B **91**, 075203 (2015).

[39] D. S. P. Tanner, M. A. Caro, S. Schulz, and E. P. O'Reilly, Phys. Rev. Materials **3**, 013604 (2019).

[40] P. N. Keating, Phys. Rev. **149**, 674 (1966).

[41] M. Blackman, The Philosophical Magazine: A Journal of Theoretical Experimental and Applied Physics **3**, 831 (1958).

[42] S. Steiger, M. Salmani-Jelodar, D. Areshkin, A. Paul, T. Kubis, M. Povolotskyi, H.-H. Park, and G. Klimeck, Phys. Rev. B **84**, 155204 (2011).

[43] K. Kim, W. R. L. Lambrecht, and B. Segall, Phys. Rev. B **53**, 16310 (1996).

[44] S. Beer, J. Jackovitz, D. Feldman, and J. Parker, Phys. Lett. A **26**, 331 (1968).

[45] T. Azuhata, T. Sota, and K. Suzuki, J. Phys.: Condens. Matter **7**, 1949 (1995).

[46] P. Y. Yu and M. Cardona, Optical properties I, *Fundamentals of Semiconductors: Physics and Materials Properties* (Springer Berlin Heidelberg, Berlin, Heidelberg, 2010), pp. 243–344.

[47] A. Mooradian and G. Wright, Solid State Commun. **4**, 431 (1966).

[48] C. Kittel, *Introduction to Solid State Physics,* 2nd ed. (Wiley, New York, 1956).

[49] R. Tubino, L. Piseri, and G. Zerbi, J. Chem. Phys. **56**, 1022 (1972).

[50] C. S. G. Cousins, Phys. Rev. B **67**, 024108 (2003).

[51] F. Grosse and J. Neugebauer, Phys. Rev. B **63**, 085207 (2001).

[52] O. Madelung (ed.), in *Semiconductors: Data Handbook,* 3rd ed. (Springer-Verlag GmbH, Heidelberg, Berlin, Heidelberg, 2003).

[53] K. Karch, J.-M. Wagner, and F. Bechstedt, Phys. Rev. B **57**, 7043 (1998).

[54] M. Hass and B. Henvis, J. Phys. Chem. Solids **23**, 1099 (1962).

[55] H. Neumann, Crystal Res. Technol. **30**, 910 (1995).

[56] D. Lockwood, G. Yu, and N. Rowell, Solid State Commun. **136**, 404 (2005).

[57] F. Bernardini, V. Fiorentini, and D. Vanderbilt, Phys. Rev. B **56**, R10024(R) (1997).

[58] P. Giannozzi, S. de Gironcoli, P. Pavone, and S. Baroni, Phys. Rev. B **43**, 7231 (1991).

[59] T. Sengstag, N. Binggeli, and A. Baldereschi, Phys. Rev. B **52**, R8613 (1995).

[60] X. Wang and D. Vanderbilt, Phys. Rev. B **75**, 115116 (2007).

[61] G. Kaczmarczyk, A. Kaschner, S. Reich, A. Hoffmann, C. Thomsen, D. J. As, A. P. Lima, D. Schikora, K. Lischka, R. Averbeck, and H. Riechert, Appl. Phys. Lett. **76**, 2122 (2000).

[62] C. Barrett and L.-W. Wang, Phys. Rev. B **91**, 235407 (2015).

[63] G. Kresse and J. Furthmüller, Phys. Rev. B **54**, 11169 (1996).

[64] S. Schulz, M. A. Caro, E. P. O'Reilly, and O. Marquardt, Phys. Rev. B **84**, 125312 (2011).

[65] D. Strauch and B. Dorner, J. Phys.: Condens. Matter **2**, 1457 (1990).

[66] Z. Sui and I. P. Herman, Phys. Rev. B **48**, 17938 (1993).

[67] A. Paul, M. Luisier, and G. Klimeck, J. Comput. Electron. **9**, 160 (2010).